Synthesis and Metabolism of the First Thia-Bilirubin

Adrianne K. Tipton,† David A. Lightner,*,† and Antony F. McDonagh*,‡

Department of Chemistry, University of Nevada, Reno, Nevada 89557-0020, and G.I. Unit and Liver Center, University of California, San Francisco, California 94143-0538

lightner@scs.unr.edu

Received November 9, 2000

A symmetrical C(10)-thiabilirubin analogue, 8,12-bis(2-carboxyethyl)-2,3,17,18-tetraethyl-7,13-dimethyl-10-thia-(21*H*,23*H*,24*H*)-bilin-1,19-dione (**1**), was synthesized from 8-(2-carboxyethyl)-2,3-diethyl-7-methyl-10*H*-dipyrrin-1-one in one step by reaction with sulfur dichloride. The thia-rubin exhibited the expected IR, UV−vis, and NMR spectroscopic properties, which are rather similar to those of mesobilirubin-XIIIα. Like bilirubin and mesobilirubin, **1** adopts an intramolecularly hydrogen-bonded conformation, shaped like a ridge-tile but with a steeper pitch. The longer C−S bond lengths and smaller bond angles at C−S−C, as compared to C−CH_2−C, lead to an interplanar angle between the two dipyrrinones of only 74°—or considerably less than that of bilirubin (∼100°). On normal- and reversed-phase chromatography, **1** is substantially less polar than bilirubin. Despite this conformational distortion, **1** is metabolized in normal rats to acyl glucuronides, which are secreted into bile. In mutant (Gunn) rats lacking bilirubin glucuronosyl transferase, **1** (like bilirubin) was not excreted in bile.

Introduction

Bilirubin is the hydrophobic, yellow-orange cytotoxic pigment of jaundice[1,2] and an important member of the linear tetrapyrrole class.[3] Its constitutional structure comprises two dipyrrinones, each joined to the same CH_2 group (Figure 1A), that have been shown to be key determinants of bilirubin conformation.[4−7] Dipyrrinones are known to be avid participants in hydrogen bonding, clinging strongly to each other to form dimers (Figure 1B)[8,9]—or to carboxylic acids.[10] For the latter, it appears nature designed dipyrrinones as natural lock and key receptors (Figure 1C).[10]

Bilirubin and its mesobilirubin relatives with ethyl groups replacing vinyls owe their peculiar lipid solubility and solution properties to a stubborn tendency of the dipyrrinones to sequester the C(8) and C(12) propionic acids. By rotating about the central C(10) CH_2 group, the dipyrrinones can come face to face with the opposing propionic acids, and by hydrogen bonding to them, the polar carboxylic acid and lactam groups are tucked inside a conformation that is shaped like a ridge-tile of a roof and is dotted with hydrophobic hydrocarbon groups on its periphery (Figure 2).[4,5] Although not rigid, these ridge-tile structures, considerably stabilized by six intramolecular hydrogen bonds, dominate the conformation of bilirubin and its analogues, and they explain its lipophilicity and poor secretion by the liver into bile.[3,11] Bilirubin can become toxic if it accumulates in the body, which does not happen to any marked degree because the pigment is converted enzymically in the liver to mono-

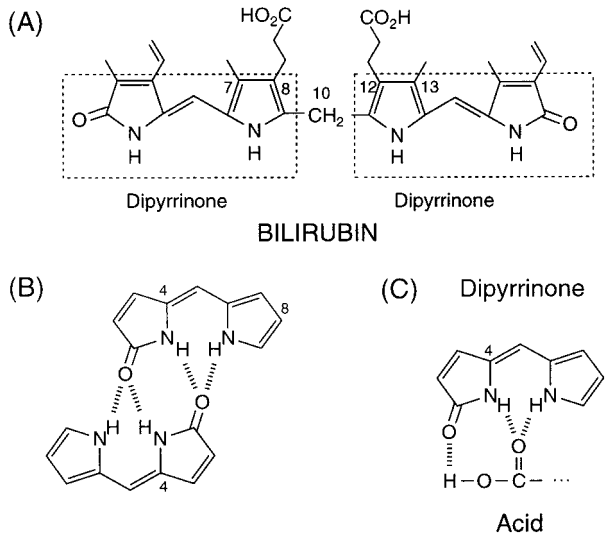

Figure 1. (A) Linear representation of bilirubin showing its two dipyrrinone chromophores conjoined to the C(10) CH_2. (B) Planar, intermolecularly hydrogen-bonded dipyrrinone. (C) Dipyrrinone hydrogen-bonded to a carboxylic acid group.

† University of Nevada.
‡ University of California.

(1) (a) McDonagh, A. F. Bile Pigments: Bilatrienes and 5,15-Biladienes. In *The Porphyrins*; Dolphin, D., Ed.; Academic Press: New York, 1979; Vol. 6, pp 293−491. (b) Schmid, R.; McDonagh, A. F. Hyperbilirubinemia. In *The Metabolic Basis of Inherited Disease*, 4th ed.; Stanbury, J. B., Wyngaarden, J. B., Fredrickson, D. S., Eds.; McGraw-Hill: New York, 1978; Chapter 51, pp 1221−1257.

(2) Berk, P. D.; Noyer, C. *Seminars Liver Dis.* **1994**, *14*, 323−394.

(3) Falk, H. *The Chemistry of Linear Oligopyrroles and Bile Pigments*; Springer-Verlag: Wien, 1989.

(4) (a) Bonnett, R.; Davies, J. E.; Hursthouse, M. B.; Sheldrick, G. M. *Proc. R. Soc. London, Ser. B* **1980**, *B36*, 3007−3011. (c) Sheldrick, W. S. *Isr. J. Chem.* **1983**, *23*, 155−166.

(5) For leading references, see: Kaplan, D.; Navon, G. *Isr. J. Chem.* **1983**, *23*, 177−186.

(6) Person, R. V.; Peterson, B. R.; Lightner, D. A. *J. Am. Chem. Soc.* **1994**, *116*, 42−59.

(7) (a) Nogales, D.; Lightner, D. A. *J. Biol. Chem.* **1995**, *270*, 73−77. (b) Dörner, T.; Knipp, B.; Lightner, D. A. *Tetrahedron* **1997**, *53*, 2697−2716.

(8) Falk, H.; Grubmayr, K.; Höllbacher, G.; Hofer, O.; Leodolter, A.; Neufingerl; Ribó, J. M. *Monatsh. Chem.* **1977**, *108*, 1113−1130.

(9) Nogales, D. F.; Ma, J.-S.; Lightner, D. A. *Tetrahedron* **1993**, *49*, 2361−2372.

(10) (a) Boiadjiev, S. E.; Anstine, D. T.; Lightner, D. A. *J. Am. Chem. Soc.* **1995**, *117*, 8727−8736. (b) Boiadjiev, S. E.; Anstine, D. T.; Maverick, E.; Lightner, D. A. *Tetrahedron: Asymmetry* **1995**, *6*, 2253−2270.

10.1021/jo001598w CCC: $20.00
Published on Web 02/13/2001

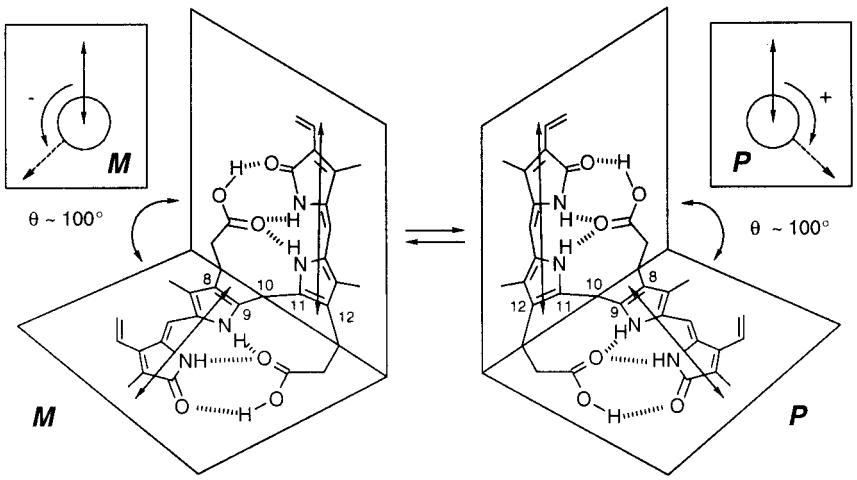

Figure 2. Interconverting intramolecularly hydrogen-bonded enantiomeric conformers of bilirubin. The double headed arrows represent the dipyrrinone long wavelength electric dipole transition moments. The relative helicities (***M***, minus or ***P***, plus) of the vectors are shown (inset) for each enantiomer. Hydrogen bonds are shown by hatched lines.

and diglucuronide metabolites that are less lipophilic and are efficiently eliminated in bile.[1,2] Translocation of bilirubin glucuronides from the liver into bile across the canalicular membrane of the hepatocyte is believed to be effected by the ATP-dependent glycoprotein MRP2 (multidrug resistance protein 2; also known as *c*-MOAT, canalicular multispecific organic anion transporter.)[12] Bilirubin itself is hydrophobic and is not excreted significantly in bile or urine.[13] Presumably, this is because of its high affinity for serum and hepatic proteins and/or because it is not transported by any of the several membrane transport proteins that facilitate the biliary excretion of other organic anions and amphipathic small molecules.

In our investigations of the importance of the 3-dimensional molecular structure of bilirubin to its metabolism, we have constructed bilirubin analogues designed to alter the pigment's lipophilicity by substitution at C(10),[14−16] the "hinge" of the ridge-tile conformation (Figure 2). For example, with a *gem*-dimethyl at C(10), the rubins become amphiphilic and easily soluble in both chloroform and methanol,[15] yet are metabolized in the usual way.[14] In contrast, with an oxo group at C(10), the pigment becomes more polar and much less soluble in chloroform than bilirubin[16]—and is excreted by the liver into bile both as a glucuronide and as the intact pigment. To alter the interplanar angle of the ridge-tile, we have designed and synthesized the first thia-bilirubin (**1**), with a sulfur atom replacing the C(10) CH_2 group. Like bilirubin, **1** (Figure 3), is predicted by molecular modeling (Sybyl) to engage in intramolecular hydrogen bonding—despite the long C−S bonds connecting the two dipyrrinones to the C(10) sulfur atom, and despite the smaller bond angles around the sulfide. In contrast, the thia-rubin without propionic acids (**2**) (Scheme 1) is expected to have solution properties like those of bilirubins without propionic acids, such as etiobilirubin-IVγ. Thia-porphyrins and thia-phlorins have been prepared previously,[17] but to our knowledge, **1** and **2** are the first examples of 10-thia-bilirubins. In the following, we describe the syntheses of **1** and **2** and the metabolic disposition of **1** in normal rats and in homozygous Gunn rats lacking bilirubin conjugating activity.

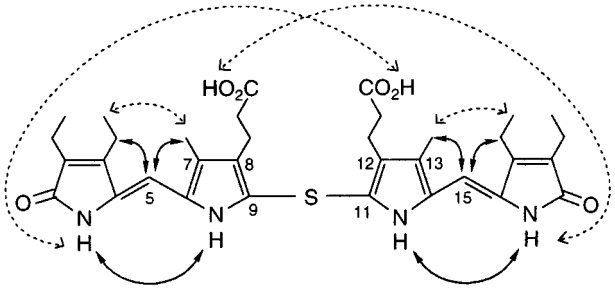

Figure 3. NOEs found for thia-rubin **1** are shown by curved, double-headed arrows. Weak NOEs are shown by curved, dashed arrows.

Results and Discussion

Synthesis. 10-Thia-mesobilirubin **1** was chosen as a synthetic target because of its expected ease of synthesis and because its parent (**3a**), with 10-CH_2, is closely related to mesobilirubin-XIIIα (**3b**). Both **3a** and **3b** are very similar to bilirubin in their chemical properties[14a] and metabolism in rats.[15,16]

Falk and Flödl[18] demonstrated some 10 years ago that a conjugated tripyrrinone could be condensed with sulfur dichloride to afford a 91% yield of a thia-hexapyrrole

(11) (a) McDonagh, A. F.; Lightner, D. A. In *Hepatic Metabolism and Disposition of Endo and Xenobiotics*; Bock, K. W., Gerok, W., Matern, S., Eds.; Falk Symposium No. 57; Kluwer: Dordrecht, The Netherlands, 1991; Chapter 5, pp 47−59.

(12) (a) Paulusma, C.; Oude Elferink, R. P. J. *J. Mol. Med.* **1997**, *75*, 420−428. (b) Jedlitscky, G.; Leier, I.; Buchholtz, U.; Hummel Eisenbeiss, J.; Burchell, B.; Keppler, D. *Biochem. J.* **1997**, *327*, 305−310.

(13) Chowdhury, J. R.; Wolkoff, A. W.; Chowdhury, N. R.; Arias, I. M. Hereditary Jaundice and Disorders of Bilirubin Metabolism. In *The Metabolic and Molecular Bases of Inherited Disease*; Scriver, C. R., Beaudet, A. L., Sly, W. S., Valle, D., Eds.; McGraw-Hill: New York, 1995; Vol. II, Chapter 67, pp 2161−2208.

(14) (a) Xie, M.; Lightner, D. A. *Tetrahedron* **1993**, *49*, 2185−2200. (b) Thyrann, T.; Lightner, D. A. *Tetrahedron Lett.* **1995**, *36*, 4345−4348. (c) Kar, A.; Lightner, D. A. *Tetrahedron* **1998**, *54*, 12671−12690.

(15) McDonagh, A. F.; Lightner, D. A. *Cell. Molec. Biol.* **1994**, *40*, 965−974.

(16) Chen, Q.; Huggins, M. T.; Lightner, D. A.; Norona, W.; McDonagh, A. F. *J. Am. Chem. Soc.* **1999**, *121*, 9253−9264.

(17) (a) Smith, K. M. *Porphyrins and Metalloporphyrins*; Elsevier: Amsterdam, 1975. (b) Latos-Grazynski, L. In *The Porphyrin Handbook*; Kadish, K. M., Smith, K. M., Guilard, R., Eds.; Academic Press: New York, 1999; Vol. 2.

(18) Falk, H.; Flödl, H. *Monatsh. Chem.* **1989**, *120*, 45−51.

Scheme 1

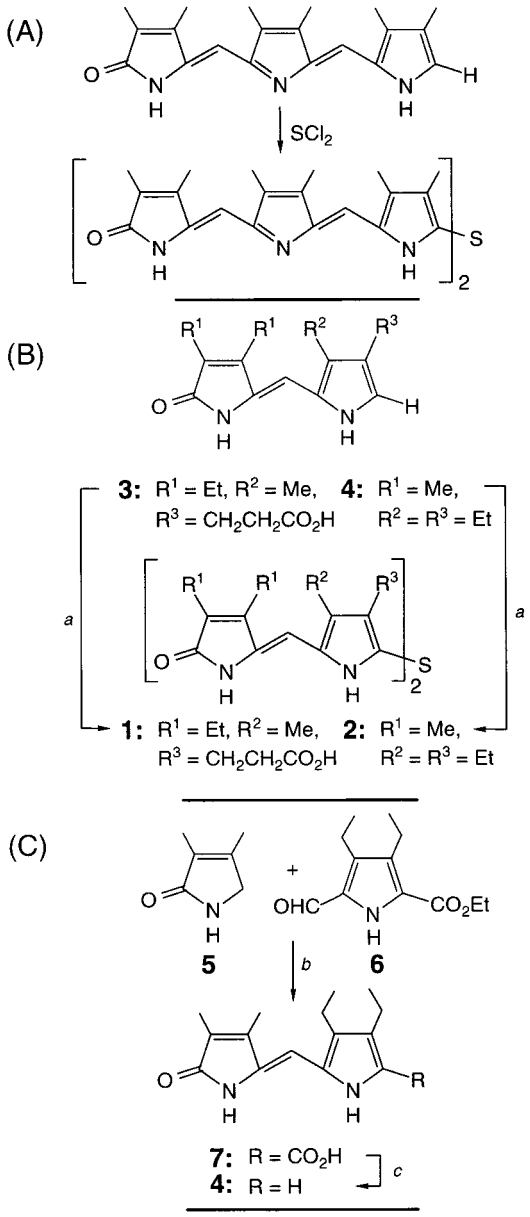

(Scheme 1A). Although a similar reaction has not been reported with dipyrrinones, we suspected that by reaction of a suitable 9-H dipyrrinone with SCl_2, we might achieve the synthesis of a thia-bilirubin. To test this hypothesis, we first attempted a condensation with readily available 9-H dipyrrinone (**4**) having only β-alkyl substituents (Scheme 1B). Dipyrrinone **4** was conveniently prepared by reaction of ethyl 3,4-diethyl-5-formylpyrrole-2-carboxylate (**6**)[19] (prepared in 88% yield by oxidation of ethyl 3,4-diethyl-5-methylpyrrole-2-carboxylate[20] with ceric ammonium nitrate)[21] with the known and easily prepared 3,4-dimethyl-1*H*-pyrrolin-2-one (**5**)[14a,b] in refluxing aqueous methanol (Scheme 1C). The initially formed 9-carboxy-dipyrrinone (**7**), obtained in 88% yield, was smoothly decarboxylated in molten KOAc−NaOAc to afford an overall 80% yield of **4**. Gratifyingly, reaction of a solution of **4** in CH_2Cl_2 with 0.5 equiv of freshly distilled SCl_2 at room temperature afforded a 65% isolated yield of **2** as a yellow-brown solid. Because we were more interested in preparing a thia-bilirubin with propionic acid groups at C(8) and C(12), we then reacted the known dipyrrinone acid (**3**)[14a] with SCl_2 to produce thia-rubin **1** in 60% yield.

Table 1. Comparison of ^{13}C NMR Chemical Shifts[a] (ppm) and Assignments of 1 and 2

	thia-rubin in DMSO-d_6		thia-rubin in $CDCl_3$	
carbon	**1**	**2**	**1**	**2**
1, 19	171.8 (171.9)	172.2	174.8 (175.0)	174.5
2, 18	125.4 (122.9)	125.0	127.0 (123.9)	126.2
2^1, 18^1	16.35 (9.15)	8.33	16.68 (10.31)	9.64
2^2, 18^2	13.75		13.84	
3, 17	146.8 (147.1)	141.6	147.8 (148.6)	141.3
3^1, 17^1	16.93 (17.15)	9.54	17.76 (18.00)	9.79
3^2, 17^2	15.65 (14.82)		15.76 (15.11)	
4, 16	130.1 (127.8)	129.0	129.3 (128.6)	129.6
5, 15	96.72 (97.70)	96.47	99.53 (100.7)	99.59
6, 14	126.3 (122.4)	128.6	126.2 (123.3)	129.0
7, 13	121.8 (122.5)	124.5	123.7 (124.4)	125.8
7^1, 13^1	9.35 (8.07)	17.19	10.46 (8.18)	18.06
7^2, 13^2		15.53		16.53
8, 12	119.5 (119.3)	119.3	123.4 (119.6)	120.8
8^1, 12^1	19.95 (19.33)	19.34	19.17 (08.76)	18.26
8^2, 12^2	34.23 (34.56)	16.66	32.15 (32.87)	16.55
8^3, 12^3	173.8 (174.1)		179.1 (179.7)	
9, 11	130.4 (130.4)	131.4	130.0 (133.4)	131.5

[a] In ppm downfield from $(CH_3)_4Si$ for 1×10^{-3} M solutions. [b]Entries in parentheses are for mesobilirubin XIIIα (**3b**) (ref 16), a bilirubin (Figure 1) analogue with ethyl groups at C(3) and C(17) and methyl groups at C(2) and C(18).

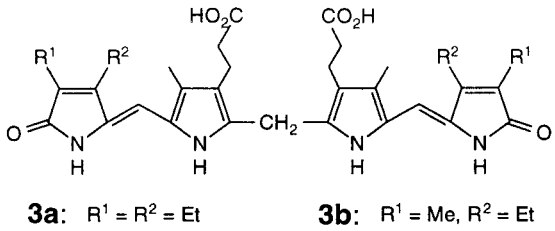

Molecular Structure. The constitutional structures of **1** and **2** follow from the previously established structures of their dipyrrinone precursors, **3** and **4** respectively. They are confirmed by their HR FAB-MS molecular weights, **1**: 634 [$M^{\cdot+}$] and **2**: 518 [$M^{\cdot+}$] and their ^{13}C NMR spectra (Table 1). Noteworthy is the absence of the ^{13}C NMR signal in **1** and **2** for the C(10) CH_2 usually found in bilirubins near 23.5 ppm in $(CD_3)_2SO$ and near 22.5 ppm in $CDCl_3$.[6] Otherwise, there are few significant differences in ^{13}C NMR chemical shifts between rubins with a C(10) CH_2 and those with C(10) replaced by S(10) (**1** and **2**): surprisingly, ring carbons 9(11) have essentially the same chemical shift, even with a sulfur substituent, and all carbons of the propionic acid chains have very similar chemical shifts, as do ring carbons 8(10), 7(13), and 3(17). However, ring carbons 2(18), 4(16), and 6(14) are more deshielded in **1** and **2** than in ordinary bilirubins, whereas the bridging carbons 5(15) are more shielded.

The ^{1}H NMR spectra of **1** and **2** are also consistent with their constitutional structures. Most significantly, the C(10) CH_2 signal seen in bilirubin and mesobilirubins near 4 ppm is absent in **1** and **2**, and the C(9) hydrogens of the starting dipyrrinones (**3** and **4**) near 6.6−6.9 ppm are also absent.

(19) Eisner, U.; Lichtarowicz, A.; Linstead, R. P. *J. Chem. Soc.* **1957**, 733.
(20) (a) Wang, C. B.; Chang, C. K. *Synthesis* **1979**, 548−549. (b) Cheng, L.; Ma, J. *Synth. Commun.* **1994**, *24*, 2771−2775.
(21) Thyrann, T.; Lightner, D. A. *Tetrahedron Lett.* **1995**, *36*, 4345−4348.

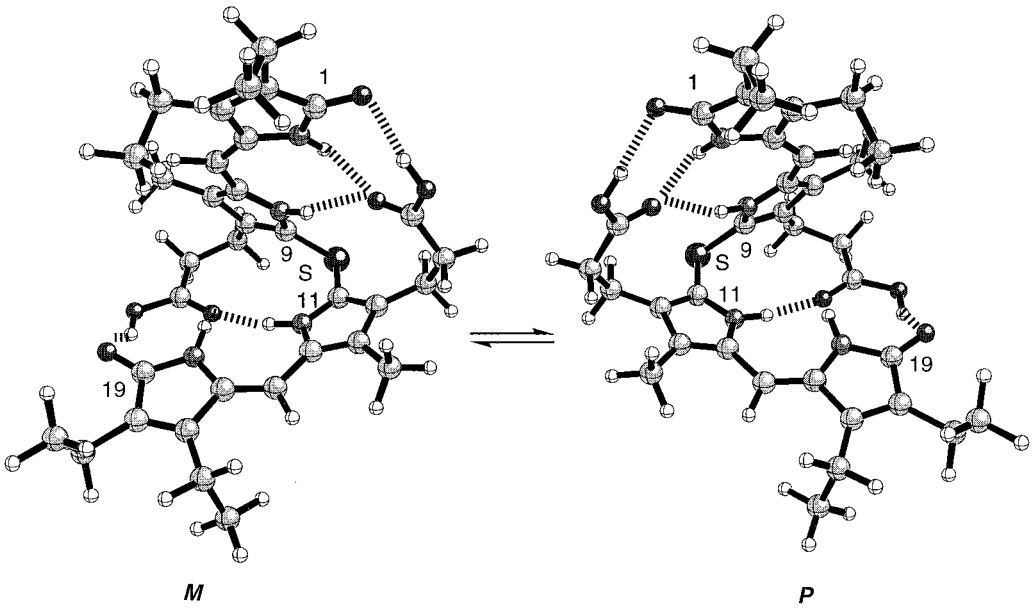

Figure 4. Ball and stick representations of the energy-minimized structures of the ***M*** and ***P*** enantiomers of thia-rubin **1**.

Table 2. ^{1}H NMR NH and COOH Chemical Shifts in $CDCl_3$ and $(CD_3)_2$ SO

	δ (ppm) $(CD_3)_2$ SO			δ ppm in $CDCl_3$		
compd	N(21),N(24)	N(22),N(23)	CO_2H	N(21),N(24)	N(22),N(23)	CO_2H
1	9.99	10.73	11.96	10.94	9.89	13.61
2	9.99	10.75		10.52	10.27	
MBR XIIIα	9.74	10.28	11.87	10.57	9.15	13.62

Conformation. ^{1}H{^{1}H}-Nuclear Overhauser effects (NOEs) are found between the lactam and pyrrole NHs of **1** and **2** in $CDCl_3$ and between the C(5)/C(15) vinyl hydrogens and the C(7)/C(13) methyls and the C(3)/C(17) ethyl group methylenes (Figure 3). These data indicate a *syn-Z* configuration at the exocyclic double bonds at C(4) and C(15). In addition, an NOE is seen between the lactam NHs and the propionic acid COOHs in **1**, indicating that they are in close proximity—as would be expected[5,7] from an intramolecularly hydrogen-bonded ridge-tile conformation (Figure 2). Further support for such a conformation for **1** in $CDCl_3$ comes from (i) the observation of an ABCX coupling pattern in the propionic acid $-CH_2-CH_2-$ segment, with coupling constants characteristic of a fixed staggered geometry,[5] and (ii) the NH chemical shifts (Table 2).[6] Concerning the latter, although the NH chemical shifts of **1** and **2** are essentially identical in $(CD_3)_2SO$ and close to those of mesobilirubin-XIIIα (**3b**), in $CDCl_3$ only **1** and **3b** have similar chemical shifts. Their NH chemical shifts in $CDCl_3$ are consistent with intramolecular hydrogen bonding, as in Figure 2. In contrast, the NH chemical shifts of **2** are consistent with intermolecular hydrogen bonding of the dipyrrinone to dipyrrinone type found in etiobilirubin-IVγ, which has only alkyl side chains, and in the dimethyl esters of bilirubin or mesobilirubin.[22] The latter are known to be dimeric (by association) in $CHCl_3$.[3,22]

In addition to the NMR spectroscopic evidence on the conformation of thia-rubin **1**, molecular dynamics calculations (Sybyl) support an intramolecularly hydrogen bonded ridge-tile conformation. Two isoenergetic ridge-tile conformations are found, corresponding to mirror image enantiomers (Figure 4). The shapes of the ridge-tiles are generally similar to those found by molecular dynamics computations and by X-ray crystallography on bilirubin and mesobilirubins. Yet, an interesting difference in shape attends the longer C(9)/C(11)−S bond lengths (∼1.8 Å) and smaller C(9)−S-C(11) bond angle (∼93°) as compared to the C(9)/C(11)−CH_2 bond length (∼1.5 Å) and C(9)−CH_2−C(11) bond angle (∼102°) of mesobilirubin or bilirubin. The ridge-tile of **1** has a smaller interplanar (or dihedral) angle (θ ∼74°) between the two dipyrrinone planes as compared to mesobilirubin or bilirubin (θ ∼100°). Thus, the ridge-tile of **1** is more closed than that of the C(10)−CH_2 parent and adapted to a roof of much steeper pitch than the bilirubin ridge-tile, as shown in Figure 5 by the edge-view Ball and Stick[3] diagrams.

Polarity and Solubility. Figure 6 shows an HPLC chromatogram of a mixture of bilirubin, thiarubin (**1**), and the analogue (**3a**) of **1** with CH_2 replacing S. The corresponding retention factors are 2.7, 4.6, and 3.7, respectively, indicating that the thiarubin is less polar than either of the two rubins and very much less polar than bilirubin. Similarly, on silica TLC **1** has an R_f ∼0.8, whereas that of mesobilirubin (**3b**) is ∼0.5 (solvent 99:1 CH_2Cl_2/MeOH by vol). Whether this is due to the more closed ridge-tile in **1** or to the replacement of the C(10) CH_2 by a (10)S, or simply to the presence of two ethyl groups (as opposed to one ethyl and one methyl) on each lactam ring is unclear. Nonetheless, thia-rubin **1**, like bilirubin and mesobilirubin, is soluble in $CHCl_3$ and insoluble in dilute aq. $NaHCO_3$ solution. Taken collectively, these characteristics are consistent with the propionic acid side chains being involved in intramolecular hydrogen bonding and unavailable for solvent interaction.

(22) Boiadjiev, S. E.; Lightner, D. A. *J. Heterocycl. Chem.* **2000**, *37*, 863−870.

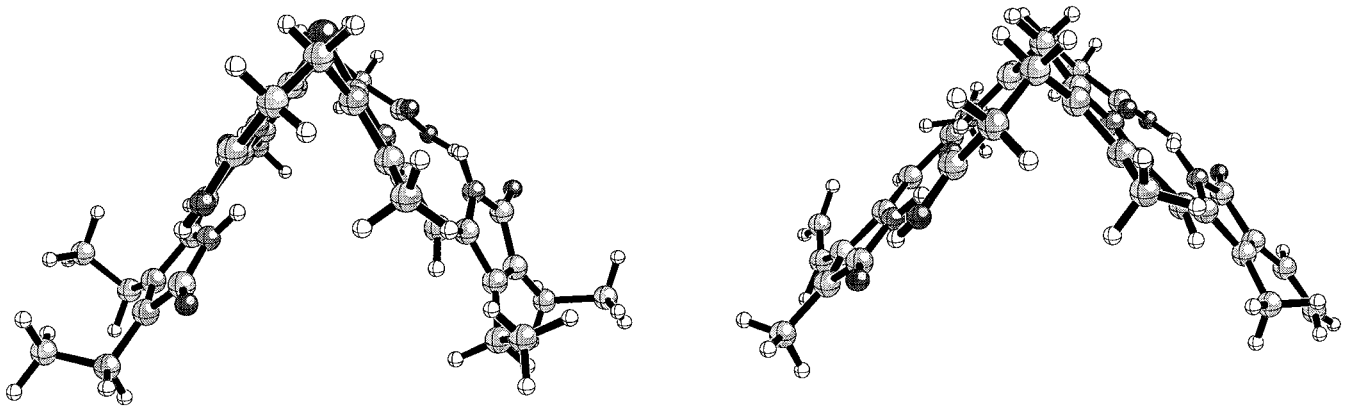

Figure 5. Edge views of the ***M***-helical ridge-tile conformations of thia-rubin **1** (left) and bilirubin (right).

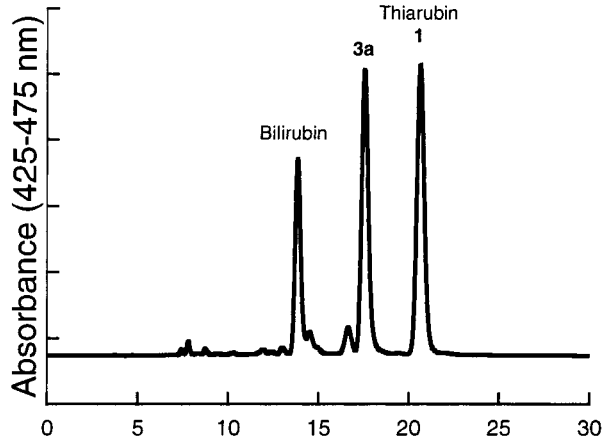

Figure 6. Reversed-phase HPLC separation of bilirubin, thiarubin **1**, and **3a**, the analogue of **1** with CH_2 replacing S.

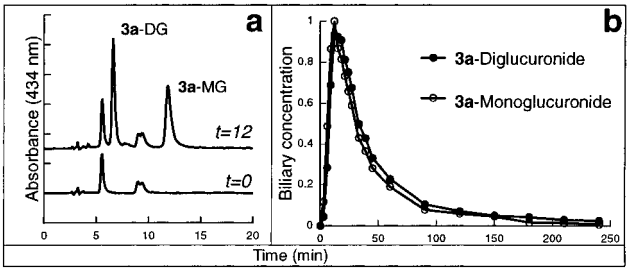

Figure 7. Metabolism and biliary excretion of **3a** in the rat. (a) HPLC chromatograms of bile collected before ($t = 0$) and 12 min after intravenous injection of **3a** (0.25 mg). At $t = 0$ the chromatogram shows the presence of bilirubin diglucuronide (main peak) and the two isomeric monoglucuronides, which are not fully resolved under the chromatographic conditions used. (b) Biliary excretion profiles for the mono- and diglucuronides of **3a**, derived from HPLC analyses of bile.

Hepatic Metabolism. Bilirubin is cleared from the circulation in healthy humans, rats, and many other mammals by the liver, where it undergoes enzymic conversion to two isomeric monoglucuronides.[1,2,13] These are partly converted by the same enzyme to bilirubin diglucuronide. The resulting mixture of three acyl glucuronides is secreted from the liver into bile. Formation of the glucuronides is catalyzed by the glucuronosyl transferase enzyme UGT1A1 (UGT1.1).[23−28] When this enzyme is absent, as in the homozygous Gunn rat,[23−25,28] bilirubin glucuronides are not formed and only very low concentrations of the parent pigment and none of its glucuronides are excreted in bile. This causes accumulation of bilirubin in the circulation and extravascular tissues. Efficient uptake of bilirubin into the liver from the circulation may require a specific organic anion transport protein located in the plasma membrane,[29] and efficient secretion of bilirubin glucuronides into bile is thought to depend on another organic anion transport protein localized in the canalicular membrane of hepatocytes.[30] The canalicular transporter has been named multidrug resistance protein two (MRP2 for human, mrp2 for rat) and canalicular multispecific organic anion transporter (cMOAT) and is a product of the ABC-transporter gene ABCC2. It is not known why bilirubin, which is an organic anion at physiologic pH, is not transported efficiently into bile by MRP2 or any of the other organic anion transporters that inhabit the canalicular membrane, but the reason may be related to the conformation, intramolecular hydrogen bonding and resulting lipophilic properties of bilirubin in vivo. Few rubins that are more lipophilic than bilirubin have previously been studied in vivo.

Compound **3a** is a symmetrical, more heavily alkylated, analogue of bilirubin. It is identical to thiarubin **1** except for the CH_2 replacing the S. Both **3a** and **1** are chromatographically less polar (more hydrophobic) than bilirubin (Figure 6). Confirming earlier observations,[15] we find that rubin **3a** is metabolized in the rat just like bilirubin (Figure 7). Thus, it is not excreted significantly in bile following its intravenous injection into homozygous Gunn rats, but is excreted rapidly as two glucuronides, presumably the mono- and di-, on similar treatment of normal rats. The ratio of the mono- to the diglucuronide in bile was ∼0.9:1 during the period of maximum excretion (based on HPLC peak areas) which is somewhat higher than the relative ratio (∼0.6−0.8:1) of the endogenous bilirubin mono and diglucuronides in

(23) Iyanagi, T.; Watanabe, T.; Uchiyama, Y. *J. Biol. Chem.* **1989**, *264*, 21302−21307.
(24) Sato, H.; Aono, S.; Kashiwamata, S.; Koiwai, O. *Biochem. Biophys. Res. Commun.* **1991**, *177*, 1161−1164.
(25) Clarke, D. J.; Keen, J. N.; Burchell, B. *FEBS Lett.* **1992**, *299*, 183−186.
(26) Ritter, J. K.; Chen, F.; Sheen, Y. Y.; Tran, H. M.; Kimura, S.; Yeatman, M. T.; Owens, I. S. *J. Biol. Chem.* **1992**, *267*, 3257−3261.
(27) Coffman, B. L.; Green, M. D.; King, C. D.; Tephly, T. R. *Mol. Pharmacol.* **1995**, *47*, 1101−1105.
(28) King, C. D.; Green, M. D.; Rios, G. R.; Coffman, B. L.; Owens, I. S.; Bishop, W. P.; Tephly, T. R. *Arch. Biochem. Biophys.* **1996**, *332*, 92−100.
(29) Zucker, S. D.; Goessling, W. *Biochim. Biophys. Acta-Biomembranes* **2000**, *1463*, 197−208.
(30) Kamisako, T.; Leier, I.; Cui, Y. H.; Konig, J.; Buchholz, U.; Hummel-Eisenbeiss, J.; Keppler, D. *Hepatology* **1999**, *30*, 485−490.

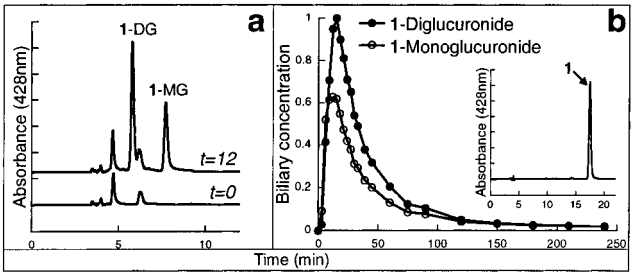

Figure 8. Metabolism and biliary excretion of **1** in the rat. (a) HPLC chromatograms of bile collected before ($t = 0$) and 12 min after intravenous injection of **1** (0.25 mg). At $t = 0$ the chromatogram shows the presence of bilirubin diglucuronide (main peak) and the two isomeric monoglucuronides, which are not fully resolved under the chromatographic conditions used. (b) Biliary excretion profiles for the mono and diglucuronides of **1**, derived from HPLC analyses of bile. The inset in panel b shows an HPLC chromatogram of the serum solution of **1** used for intravenous injection.

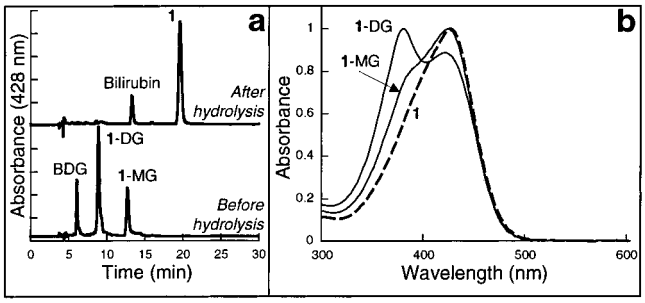

Figure 9. (a) Hydrolysis of glucuronides of **1** with β-glucuronidase. A sample of bile collected ~15 min after intravenous injection of a rat with **1** was chromatographed by HPLC before and after treatment with β-glucuronidase. BDG indicates bilirubin diglucuronide. Under the chromatographic conditions used, bilirubin monoglucuronide peaks overlapped the peak of **1**-diglucuronide (**1**-DG). (b) Absorption spectra of **1** and its mono (**1**-MG) and diglucuronide (**1**-DG). The spectra are normalized to maximum absorbance above 350 nm.

the bile of the rats used for the study. Despite its substantially greater lipophilicity, thiarubin **1** behaved almost identically to bilirubin and to rubin **3a** in vivo in the rat (Figure 8). After being injected intravenously, no significant excretion of the pigment in bile was evident in Gunn rats, but prompt excretion of two metabolites was seen in normal rats. Both metabolites were more polar than the parent pigment. They had absorption spectra resembling that of the parent pigment (Figure 9b) and were hydrolyzed by 1.0 M NaOH and by β-glucuronidase to the parent compound (**1**) (Figure 9a). On this evidence, coupled with the fact that they were not formed in Gunn rats, we conclude that the metabolites are the mono- and diglucuronide of thiarubin. The ratio of mono- to diglucuronide in bile was ~0.7:1 during the period of maximum excretion (based on HPLC peak areas). The most polar of the two metabolites, presumably the diglucuronide, ran close to bilirubin monoglucuronides on HPLC. The least polar (presumably the monoglucuronide) is relatively lipophilic since its HPLC retention time is similar to that of unconjugated bilirubin. Since unconjugated bilirubin is not excreted in bile whereas thiarubin monoglucuronide is excreted, polarity does not seem to be the sole determinant of canalicular secretion.

Our results show that replacing the central methylene (CH_2) group of a close analogue of bilirubin by sulfur, thereby tightening the pitch of the favored ridge-tile conformation and increasing the lipophilicity of the molecule, does not markedly hinder its glucuronidation in vivo by UGT1A1. Thiarubin, **1**, like bilirubin and rubin **3a**, is taken up rapidly from the circulation into the liver, but is not transported into bile by mrp2 or other canalicular membrane transporters. In contrast, its glucuronides, like those of bilirubin and **3a**, are secreted promptly in bile. Presumably, the mechanisms involved in the hepatic uptake of **1** and **3a** and in the biliary excretion of their glucuronides are the same as those involved in the uptake of bilirubin and excretion of its glucuronides.

Experimental Section

NMR spectra were obtained at 300 and 500 MHz in $CDCl_3$ (unless otherwise noted), and chemical shifts were reported in ppm. UV−vis spectral data were determined in spectral-grade solvents (Aldrich or Fisher). HRMS were obtained at the University of Minnesota Mass Spectrometry Service Laboratory, Minneapolis, MN, and GC−MS analyses were carried out on a capillary gas chromatograph (30 m DB-1 column) equipped with a mass selective detector. Combustion analyses were done by Desert Analytics, Tucson, AZ. Analytical thin-layer chromatography (TLC) was carried out on J. T. Baker silica gel IB-F plates (125 μm layer); radial chromatography was carried out on Merck silica gel PF_{254} with $CaSO_4$, preparative layer grade. For HPLC analyses, detection was in the range of ~410−460 nm, depending on the pigments being analyzed, and the column was a Beckman-Altex ultrasphere-IP 5 μm C-18 ODS column (25 × 0.46 cm) fitted with a similarly packed precolumn (4.5 × 0.46 cm). The flow rate was 0.75−1.0 mL/minute, the elution solvent was 0.1 M di-*n*-octylamine acetate in 2−8% aqueous methanol,[14] and the column temperature ~34 °C. Di-*n*-octylamine was obtained from Aldrich and HPLC grade MeOH from Fisher, β-glucuronidase (*E. coli* Type VII-A, 1000 units/vial), phosphatidyl choline (Type XV-E), cholesterol, taurine, sodium cholate and human serum albumin (defatted) were obtained from Sigma. All solvents and reagents, unless otherwise specified, were purchased from Acros, Aldrich, or Fisher. The ball and stick drawings were created from the atomic coordinates of the molecular dynamics structures using the Müller and Falk "Ball and Stick" program (Cherwell Scientific, Oxford, UK) for Macintosh. The molecular dynamics calculations were carried out on either Evans and Sutherland or Silicon Graphics workstations using Sybyl 6.1 or Sybyl 6.5 with Gasteiger-Hückel calculation of electrostatic charge. Homozygous male Gunn rats, weighing 300−400 g, were obtained from our own colony and Sprague−Dawley male rats, weight 370−520 g, were obtained from local commercial vendors. In vivo studies were done in a windowless room under safe lights, as described elsewhere.[31]

(4*Z*,15*Z*)-8,12-Bis(2-carboxyethyl)-7,13-dimethyl-2,3,17,18-tetraethyl-10-thia-(21*H*,23*H*,24*H*)-1,19-dioxobilin (1). 2-Ethylneoxanthobilirubic acid (**3**)[14a] (100 mg, 0.33 mmol) was dissolved in CH_2Cl_2 (30 mL); then, freshly distilled sulfur dichloride (11 μL, 17.6 mg, 0.17 mmol) was added, and the solution was stirred for 3 h. A second portion of SCl_2 was added (11 μL,17.6 mg, 0.17 mmol), and the reaction was allowed to stir for an additional 3 h, after which time the reaction was quenched with water. The organic layer was separated and washed with water (2 × 20 mL) and then aqueous sodium bicarbonate solution (10%, 2 × 50 mL). It was dried (anhyd Na_2SO_4), filtered, and evaporated (rotovap). The residue was flash vacuum chromatographed with CH_2Cl_2 as eluent to afford thia-rubin **1** (63 mg, 60% yield): mp of 268−270 °C; IR (KBr) ν (cm^{-1}) 3401, 2966, 2919, 2872, 2366, 2319, 1701, 1684, 1625, 1390, 1219, 1008, 984;

(31) Brower, J. O.; Norona, W.; McDonagh, A. F.; Lightner, D. A. *Tetrahedron* **2000**, *56*, 7869−7883.

^{1}H NMR ($(CD_3)_2SO$) δ 1.03 (t, J = 7.5 Hz, 6H), 1.10 (t, J = 7.5 Hz, 6H), 1.99 (s, 6H), 2.01 (q, J = 7.5 Hz, 4H), 2.25 (q, J = 7.5 Hz, 4H), 2.51 (t, J = 8.5 Hz, 6H), 2.66 (t, J = 8.5 Hz, 6H), 5.90 (s, 2H), 9.90 (brs, 2H), 10.75 (brs, 2H), 11.96 (brs, 2H) ppm; ^{1}H NMR ($CDCl_3$) δ 1.09 (t, J = 7.5 Hz, 6H), 1.15 (t, J = 7.5 Hz, 6H), 2.16 (s, 6H), 2.33 (s, 6H), 2.48 (q, J = 7.5 Hz, 4H), 2.6, 2.8, 2.9, 3.4 (4H, ABCX), 6.01 (s, 2H), 9.89 (brs, 2H), 10.94 (brs, 2H), 13.61 (brs, 2H) ppm; ^{13}C NMR see Table 1; UV ϵ_{430}^{max} 45 400 (acetone), ϵ_{430}^{max} 45 900 (benzene), ϵ_{438}^{max} 45 500 (chloroform), ϵ_{385}^{max} 37 400, ϵ_{419}^{max} 39 800 (dimethyl sulfoxide), ϵ_{390}^{max} 38 000, ϵ_{428}^{max} 46 500 (methanol); FAB-HRMS (MNBA matrix + PEG 400 + Na ref) found 657.2756 ($M^{\bullet+}$ + Na), calcd for $C_{34}H_{42}N_4O_6$ (634.2825) + Na (22.9898) = 657.2723 amu. Anal. Calcd for $C_{34}H_{42}N_4O_6S$ (634.8): C, 64.33; H, 6.67; N, 8.83. Anal. Calcd for $C_{34}H_{42}N_4O_6S\cdot H_2O$ (652.8): C, 62.56; H, 6.79; N, 8.58. Found: C, 62.71; H, 6.46; N, 8.49.

(4*Z*,15*Z*)-8,7,12,13-Tetraethyl-2,3,17,18-tetramethyl-10-thia-(21*H*,23*H*,24*H*)-1,19-dioxobilin (2). 2,3-Dimethyl-7,8-diethyl-(10*H*)-dipyrrin-1-one (**4**) (100 mg, 0.41 mmol) was dissolved in CH_2Cl_2 (30 mL); then, freshly distilled sulfur dichloride (13 μL, 20.4 mg, 0.20 mmol) was added, and the solution was stirred for 3 h. A second portion of sulfur dichloride (6 μL, 9.6 mg, 0.09 mmol) was added, and the reaction was allowed to stir for an additional 3 h before quenching with water. The organic layer was separated and washed with water (2 × 50 mL) and then with sodium bicarbonate solution (10%, 2 × 50 mL). The organic layer was dried (anhyd Na_2SO_4), filtered, and evaporated (rotovap). The residue was flash vacuum chromatographed with CH_2Cl_2−MeOH (98:2 by vol) as eluent to afford 69 mg, 65% yield, of the desired thia-rubin **2**: mp 246−248 °C dec; IR (KBr) ν 3342, 2954, 2907, 2860, 2343, 1672, 1625, 1443, 1378, 1225, 1166, 1102, 1043, 943, 826, 749, 120, 690 cm^{-1}; ^{1}H NMR ($(CD_3)_2SO$) δ 0.77 (t, J = 7.5 Hz, 6H), 1.00 (t, J = 7.5 Hz, 6H), 1.76 (s, 6H), 2.03 (s, 6H), 2.34 (q, J = 7.5 Hz, 6H), 2.62 (t, J = 7.5 Hz, 6H), 5.86 (s, 2H), 9.99 (brs, 2H), 10.73 (brs, 2H) ppm; ^{1}H NMR ($CDCl_3$) δ 1.15 (t, J = 7.5 Hz, 6H), 1.17 (t, J = 7.5 Hz, 6H), 1.74 (s, 6H), 1.94 (s, 6H), 2.53 (q, J = 7.5 Hz, 4H), 2.71 (t, J = 7.5 Hz, 6H), 5.90 (s, 2H), 10.27 (brs, 2H), 10.52 (brs, 2H) ppm; ^{13}C NMR see Table 1; UV−vis ϵ_{374}^{max} 52 400 (acetone), ϵ_{380}^{max} 61 100 (benzene), ϵ_{379}^{max} 58 100 (chloroform), ϵ_{382}^{max} 36 600, ϵ_{421}^{max} 38 500 (dimethyl sulfoxide), ϵ_{383}^{max} 35 100, ϵ_{423}^{max} 32 000 (methanol); FAB-HRMS (MNBA matrix + PEG 400 + Na ref) found 541.2629 ($M^{\bullet+}$ + Na), calcd for $C_{34}H_{38}N_4O_2S$ (518.2715) + Na (22.9898) = 541.2613 amu. Anal. Calcd for $C_{30}H_{38}N_4O_2S$ (518.7): C, 69.47; H, 7.38; N, 10.80; S, 6.20. Anal. Calcd for $C_{30}H_{38}N_4O_2S\cdot{}^1/_2H_2O$ (527.7): C, 68.28; H, 7.45; N, 10.62; S, 6.10. Found: C, 68.63; H, 7.20; N, 10.30; S 6.13.

2,3-Dimethyl-7,8-diethyl-(10*H*)-dipyrrin-1-one (4). In a 250 mL round-bottom flask were combined 3,4-dimethyl-1*H*-pyrrolin-2-one (**5**)[14a] (5.5 g, 50 mmol), ethyl 3,4-diethyl-5-formylpyrrole-2-carboxylate (**6**)[20] (11.0 g, 50 mmol), and methanol (270 mL). Aqueous potassium hydroxide (4 M, 178 mL) was added, and the solution was heated at reflux for 2 h. The methanol was then removed (rotovap), and the solution was cooled in an ice bath. Concentrated hydrochloric acid was added until the solution became acidic and a precipitate formed. After being cooled for 1 h, the precipitate was isolated by filtration and dried to afford 12.5 g (88% yield) of dipyrrinone 9-carboxylic acid **7**. This was added to a melt of sodium acetate trihydrate (55 g, 0.4 mol) and potassium acetate trihydrate (58 g, 0.4 mol) at 140 °C, and the mixture was heated to 160 °C for 30 min, or until the evolution of CO_2 ceased. After cooling, water (100 mL) was added to the cooled mixture, and solids were removed by filtration and washed copiously with water to dissolve any residual salts. The dipyrrinone was then passed through a short pad of silica gel (under aspirator pressure) using CH_2Cl_2−MeOH (97:3 by vol) as eluent to afford 8.3 g, 80% yield of **4**: mp 195−8 °C; IR (KBr) ν 3367, 3193, 3150, 2953, 2910, 1648, 1507, 1398, 1267, 1174, 1117, 939, 793, 750, 717, 690 cm^{-1}; ^{1}H NMR ($CDCl_3$) δ 1.13 (t, J = 7.8 Hz, 3H), 1.21 (t, J = 7.8 Hz, 3H), 1.94 (s, 3H), 2.13 (s, 3H), 2.52 (q, J = 7.8 Hz, 2H), 2.82 (q, J = 7.8 Hz, 2H), 6.20 (s, 1H), 6.86 (d, J = 2.0 Hz, 1H), 10.41 (brs, NH), 11.05 (brs, NH) ppm; ^{13}C NMR ($CDCl_3$) δ 8.52, 10.18, 15.10, 16.78, 17.93, 18.47, 101.36, 120.54, 123.83, 124.35, 126.00, 129.90, 130.41, 142.62, 174.5 ppm; UV−vis ϵ_{278}^{max} 28 700 (acetone), ϵ_{394}^{max} 29 100 (benzene), ϵ_{392}^{max} 27 000 (chloroform), ϵ_{399}^{max} 28 500, (dimethyl sulfoxide), ϵ_{398}^{max} 28 100 (methanol). Anal. Calcd for $C_{15}H_{20}N_2O$ (244): C, 73.74; H, 8.25; N, 11.47. Found: C, 73.93; H, 8.19; N, 11.19.

Ethyl 3,4-Diethyl-5-formylpyrrole-2-carboxylate (6). We used a procedure modified from Thyrann and Lightner.[21] Ethyl 3,4-diethyl-5-methylpyrrole-2-carboxylate[20] (8.4 g, 0.04 mol) was dissolved in methanol (200 mL) in a 500 mL round-bottom flask. Ceric ammonium nitrate (88 g, 0.16 mol) was added in portions, while making sure each portion was dissolved completely before the next was added. The solution was stirred for 3 h and then poured into ice water (2 L). The precipitated oil was extracted with methylene chloride (200 mL), washed with water (100 mL), dried over anhyd Na_2SO_4, and filtered. The solvent was removed (rotovap), and residual oil was crystallized from ethanol−water to afford 7.8 g (88% yield) of aldehyde **6**: mp 49−50 °C (lit.[19] mp 53 °C); IR (KBr) ν 3259, 2964, 2921, 2867, 1692, 1666, 1547, 1479, 1462, 1364, 1338, 1253, 1132, 1021 cm^{-1}; ^{1}H NMR ($CDCl_3$) δ 1.15 (t, J = 7.3 Hz, 3H), 1.23 (t, J = 7.3 Hz, 3H), 1.37 (t, J = 7.3 Hz, 3H), 2.73 (q, J = 7.3 Hz, 4H), 4.36 (q, J = 7.3 Hz, 2H), 9.52 (brs, 1H), 9.77 (s, 1H) ppm; ^{13}C NMR ($CDCl_3$) δ 14.01, 15.22, 16.13, 17.41, 18.62, 60.81, 124.11, 130.04, 132.51, 137.2, 160.01, 178.99 ppm.

Acknowledgment. We thank the National Institutes of Health (HD-17779, DK 26307, and GM 36633) for support of this research. We thank Ms. Wilma Norona and Lucita Palma for expert surgical and analytical assistance and Dr. Michael Huggins for generating the ball and stick drawings of Figures 4 and 5.

JO001598W